

DEPARTMENT OF MECHANICAL ENGINEERING AND MECHANICS
SCHOOL OF ENGINEERING
OLD DOMINION UNIVERSITY
NORFOLK, VIRGINIA 23508

A TAYLOR-GALERKIN FINITE ELEMENT ALGORITHM FOR
TRANSIENT NONLINEAR THERMAL-STRUCTURAL ANALYSIS

N87-10406

Unclassified
44238

By

Earl A. Thornton, Principal Investigator

and

Pramote Dechaumphai, Research Associate

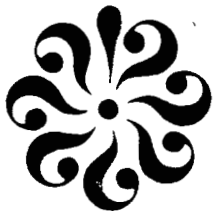
Progress Report
For the period ending January 1, 1986

Prepared for the
National Aeronautics and Space Administration
Langley Research Center
Hampton, Virginia 23665

Under
Research Grant NSG-1321
Allan R. Weiting, Technical Monitor
LAD-Aerostructural Loads Branch

Submitted by the
Old Dominion University Research Foundation
P. O. Box 6369
Norfolk, Virginia 23508

(NASA-CR-177064) A TAYLOR-GALERKIN FINITE
ELEMENT ALGORITHM FOR TRANSIENT NONLINEAR
THERMAL-STRUCTURAL ANALYSIS Progress
Report, Period ending 1 Jan. 1986 (Old
Dominion Univ.) 12 p



April 1986

A TAYLOR-GALERKIN FINITE ELEMENT ALGORITHM FOR TRANSIENT
NONLINEAR THERMAL-STRUCTURAL ANALYSIS

Earl A. Thornton* and Pramote Dechaumphai**
Old Dominion University
Norfolk, Virginia

Abstract

A Taylor-Galerkin finite element method for solving large, nonlinear thermal-structural problems is presented. The algorithm is formulated for coupled transient and uncoupled quasistatic thermal-structural problems. Vectorizing strategies ensure computational efficiency. Two applications demonstrate the validity of the approach for analyzing transient and quasistatic thermal-structural problems.

Nomenclature

a	propagation speed, eq. (16)
A	element area
c	fictitious damping constant, eq. (3a)
C_{ij}	elastic constants
c_v	specific heat at constant volume
D	diffusion coefficient, eq. (16)
f_x, f_y	body forces per unit volume
E, F	stresses or heat fluxes
H	"load" vector, eq. (1a)
k_x, k_y	thermal conductivities
n, m	components of unit normal surface vector
$[M]$	mass matrix
$[N(x,y)]$	element interpolation functions
$[N(s)]$	interpolation functions on an element edge
q_x, q_y	heat flux components
Q	volumetric heating rate
$\{R_i\}$	load vectors, eq. (14)
t	time
Δt	time step
T	temperature
T_0	reference temperature for zero stress

u, v	displacement components
\dot{u}, \dot{v}	velocity components
U	typical unknown
x, y	coordinate directions
β_{ij}	thermal-mechanical coupling coefficients, eq. (1c)
ρ	density
θ	interpolation parameter
$\sigma_x, \sigma_y, \tau_{xy}$	stress components

Subscripts

D	constant element quantity
S	constant surface quantity
n	time step index

Superscript

n	time step index
-----	-----------------

Introduction

The determination of the structural response induced by thermal effects is an important factor in many aerospace structural designs. Extreme aerodynamic heating on advanced aerospace vehicles may produce severe thermal stresses that can reduce operational performance or even damage structures. The performance of laser devices can be degraded by thermal distortions of mirror surfaces. The thermal environment in space may cause orbiting structures to distort beyond operational tolerances. To predict the structural response accurately, effective numerical techniques capable of both thermal and structural analyses are required. The finite element method has been found to be particularly suited for such analyses due to its capability to model complex geometry and to perform both thermal and structural analyses.

Algorithms required for analyzing thermally-induced structural behavior depend on the rate at which structural temperatures vary with time. When temperatures change rapidly the analyses are strongly coupled, and thermal-structural interactions occur that mandate simultaneous solution of the thermal-structural equations. Temperature changes can occur rapidly due to propagation of thermoelastic waves, during vibration induced by periodic variations of temperature fields, due to thermal shocks and in similar circumstances. These types of problems may involve resolving wave-

* Professor, Department of Mechanical Engineering and Mechanics, Senior Member AIAA

** Research Associate, Department of Mechanical Engineering and Mechanics, Member AIAA

like details of the time dependent response for complex structures. Moreover, if the mechanical deformation terms in the heat transfer energy equation are retained, the equations are inherently non-linear even in the material's elastic range. There is a need for effective finite element solution algorithms that can solve large nonlinear transient problems efficiently using new vector or parallel computing technology.

In the most common approach to determining structural responses induced by thermal effects, the thermal-structural analyses are assumed uncoupled, and the structural analysis is assumed quasistatic. The uncoupled assumption means that mechanical deformation terms in the heat transfer energy equation are neglected. The quasistatic assumption means that inertia terms in the structural equations of motion are neglected. The practical effect of these assumptions is that the heat transfer analysis can be performed first, and the resulting temperatures can be used as input to a subsequent stress analysis. This approach works well when temperatures change slowly as occurs, for example, in structures subjected to aerodynamic heating. Under these circumstances, the uncoupled, quasistatic idealization provides an effective approach for finite element thermal-structural analysis.

The purpose of this paper is to present a Taylor-Galerkin finite element method for solving large, nonlinear transient thermal-structural problems. The method is an application of a Taylor-Galerkin algorithm recently developed to solve the conservation equations of inviscid, compressible flow¹⁻². In the flow problem, the algorithm is used to solve the highly nonlinear Euler equations that includes capturing shock discontinuities in the flow field. Finite element models of flow problems usually are quite large with the number of equations typically in the range from 3,000 to 100,000 or more. Thus, the algorithm appears to have desirable attributes that will make it effective for large nonlinear, transient thermal-structural problems.

The formulation of nonlinear thermal-structural problems will be presented first, then the Taylor-Galerkin algorithm will be described. Next, explicit evaluation of the finite element integrals is described. Then the programming strategy for a vector computer implementation of the algorithm is described. Finally, results from two thermal-structural applications are presented.

Thermal-Structural Formulations

Coupled Thermal-Structural Analyses

The nonlinear coupled thermal-structural equations for a two-dimensional continuum³ can be written in the form

$$\frac{\partial \{U\}}{\partial t} + \frac{\partial \{E\}}{\partial x} + \frac{\partial \{F\}}{\partial y} = \{H\} \quad (1a)$$

where $\{U\}$ is the vector of unknowns, $\{E\}$ and $\{F\}$ are vectors of stresses and heat fluxes, and $\{H\}$ is a "load" vector. For coupled thermal-structural analyses a classical form of coupling is assumed in the equation for illustrative purposes, although more general thermal-structural coupling is permitted.

$$\{U\} = \begin{Bmatrix} u \\ v \\ \dot{u} \\ \dot{v} \\ \rho u \\ \rho c_v T \end{Bmatrix}, \quad \{E\} = \begin{Bmatrix} 0 \\ 0 \\ -\sigma_x \\ -\tau_{xy} \\ q_x \end{Bmatrix}, \quad \{F\} = \begin{Bmatrix} 0 \\ 0 \\ -\tau_{xy} \\ -\sigma_y \\ q_y \end{Bmatrix} \quad (1b)$$

$$\{H\} = \left\{ \begin{array}{l} \dot{u} \\ \dot{v} \\ \rho f_x \\ \rho f_y \\ T \left[\beta_{11} \frac{\partial u}{\partial x} + \frac{1}{2} \beta_{12} \left(\frac{\partial u}{\partial y} + \frac{\partial v}{\partial x} \right) + \beta_{22} \frac{\partial v}{\partial y} \right] + Q \end{array} \right\} \quad (1c)$$

where u and v are the displacements, ρ is the density, \dot{u} and \dot{v} are the velocities, c_v is the specific heat and T is the temperature; σ_x , σ_y , τ_{xy} are the stress components; q_x , q_y are the heat fluxes; f_x , f_y are body force components per unit volume; β_{11} , β_{12} , β_{22} are coefficients that depend on the coefficients of thermal expansion, and Q is the internal heat generation rate per unit volume. The first two equations in eq. (1) define the velocity components, the third and fourth equations are the equations of motion, and the fifth equation represents conservation of energy. The term with the square brackets in the last line of $\{H\}$ represents the classical nonlinear form of thermal-structural coupling³.

The structural and thermal equations are written in the form of eq. (1) to resemble the conservation equations of fluid flow. In the fluid context, the components of $\{U\}$ are called the conservation variables, and the components of $\{E\}$ and $\{F\}$ are fluxes of mass, momentum and energy across the faces of a control volume. In the thermal-structural context, the components of U may also be regarded as conservation variables. The stress components of $\{E\}$ and $\{F\}$ now represent tractions on surfaces of the control volume; however, q_x and q_y still represent heat fluxes across surfaces of the control volume.

In formulating the constitutive equations, highly nonlinear relations between stresses,

strains and temperatures are permitted as well as nonlinear relations between heat fluxes, temperatures and temperature gradients. Anisotropic materials can be accommodated as well. For simplicity, simple constitutive relations for linear, elastic orthotropic materials will be illustrated. The stress-strain relations for an orthotropic material are expressed as

$$\begin{Bmatrix} \sigma_x \\ \sigma_y \\ \tau_{xy} \end{Bmatrix} = \begin{Bmatrix} C_{11} & C_{12} & 0 \\ C_{21} & C_{22} & 0 \\ 0 & 0 & C_{33} \end{Bmatrix} \begin{Bmatrix} \frac{\partial u}{\partial x} \\ \frac{\partial v}{\partial y} \\ \frac{1}{2} \left(\frac{\partial u}{\partial y} + \frac{\partial v}{\partial x} \right) \end{Bmatrix} + (T - T_0) \begin{Bmatrix} \beta_{11} \\ \beta_{22} \\ \beta_{12} \end{Bmatrix} \quad (2a)$$

where C_{ij} are elastic constants, and T_0 is the reference temperature for zero stress. The heat fluxes are expressed by Fourier's law,

$$q_x = -k_x \frac{\partial T}{\partial x} \quad (2b)$$

$$q_y = -k_y \frac{\partial T}{\partial y}$$

where k_x , and k_y are the thermal conductivities.

Quasistatic Thermal-Structural Analysis

When temperatures change slowly, the inertia terms in the structural equations of motion can be neglected. This means that the first two equations in Eq. (1) are not required. However, even for the quasistatic case, the equations will be solved using a time-marching scheme. To retain the thermal-structural equations in a form suitable for time-marching, the components of eq. (1a) are written as

$$\{U\} = \begin{Bmatrix} cu \\ cv \\ pc_v T \end{Bmatrix}, \quad \{E\} = \begin{Bmatrix} -\sigma_x \\ -\tau_{xy} \\ q_x \end{Bmatrix}, \quad \{F\} = \begin{Bmatrix} -\tau_{xy} \\ -\sigma_y \\ q_y \end{Bmatrix} \quad (3a)$$

where c is a fictitious damping constant that is used to facilitate time marching to a steady-state quasistatic solution. The new load vector is

$$H = \begin{Bmatrix} pf_x \\ pf_y \\ Q \end{Bmatrix} \quad (3b)$$

The stress and heat flux components have been defined in eq. (2).

Boundary and Initial Conditions

Equations (1) and (3) are solved subject to appropriate initial and boundary conditions. The initial conditions consist of specifying the distributions of the conservation variables (U) at time zero. The structural boundary conditions consist of specifying the displacements or surface tractions at all points on the boundary. The thermal boundary conditions consist of specifying temperatures or heat fluxes at all points on the boundary. Convective and radiation boundary conditions are incorporated through heat fluxes.

TAYLOR-GALERKIN ALGORITHM

The solution domain D is divided into an arbitrary number of elements of r nodes each. Figure 1 shows the thermal and structural models. The same finite element model is used for the thermal and structural analyses. The figure shows typical quadrilateral elements ($r=4$) used in this paper. For simplicity, the finite element formulation will be given for a single scalar equation.

$$\frac{\partial u}{\partial t} + \frac{\partial E}{\partial x} + \frac{\partial F}{\partial y} = H \quad (4)$$

where the variables u , E , F and H are analogous to the corresponding vector quantities in eq. (1). Let $\{u\}^n$ denote the element nodal values of the variable $u(x,y,t)$ at time t_n . The time step Δt spans two typical times t_n and t_{n+1} in the transient response. The computation proceeds through two time levels, $t_{n+1/2}$ and t_{n+1} . At time level $t_{n+1/2}$, values for u that are constant within each element are computed explicitly. At time level t_{n+1} , the constant element values computed at the first time level are used to compute nodal values for u . In the time level t_{n+1} computations, element contributions are assembled to yield the global equations for nodal unknowns. The resulting equations are approximately diagonalized to yield an explicit algorithm.

Time Level $t_{n+1/2}$

To advance the solution to time level $t_{n+1/2}$, a truncated Taylor series yields

$$u(x, y, t_{n+1/2}) = u(x, y, t_n) + \frac{1}{2} \Delta t \frac{\partial u}{\partial t}(x, y, t_n). \quad (5)$$

Then eq. (4) is introduced on the right hand side of eq. (5) so that

$$u(x, y, t_{n+1/2}) = u(x, y, t_n) - \frac{1}{2} \Delta t \left[\frac{\partial E}{\partial x}(x, y, t_n) + \frac{\partial F}{\partial y}(x, y, t_n) \right] + \frac{1}{2} \Delta t H(x, y, t_n) \quad (6)$$

At time level $t_{n+1/2}$, the dependent variable $u(x, y, t_{n+1/2})$ is assumed to have a constant value $u_D^{n+1/2}$ within an element.

At time level t_n in the response u , E , F and H vary within an element and are interpolated from nodal values. Thus, the following spatial approximations are used within an element.

$$u(x, y, t_{n+1/2}) = u_D^{n+1/2}. \quad (7a)$$

$$u(x, y, t_n) = [N(x, y)]\{u\}^n \quad (7b)$$

$$E(x, y, t_n) = [N(x, y)]\{E\}^n \quad (7c)$$

$$F(x, y, t_n) = [N(x, y)]\{F\}^n \quad (7d)$$

$$H(x, y, t_n) = [N(x, y)]\{H\}^n \quad (7e)$$

where $[N(x, y)]$ denotes element interpolation functions and $\{u\}^n$ is a vector of the element nodal quantities. The equations for $u_D^{n+1/2}$ for each element are derived by the method of weighted residuals⁴. The spatial approximations given in eq. (7) are introduced into eq. (6) to give a residual; the result is multiplied by a weighting function which in this case is unity. Finally, the weighted residual is integrated over the area A of the element. The result is,

$$A u_D^{n+1/2} = \int_A [N] dA \{u\}^n - \frac{\Delta t}{2} \int_A \left[\frac{\partial N}{\partial x} \right] dA \{E\}^n - \frac{\Delta t}{2} \int_A \left[\frac{\partial N}{\partial y} \right] dA \{F\}^n + \frac{\Delta t}{2} \int_A [N] dA \{H\}^n. \quad (8)$$

With eq (8), the dependent variable $u_D^{n+1/2}$ for each element can be computed explicitly using nodal values for u , E , F and H from the previous time t_n . A later section will discuss the evaluation of the three integrals that appear on the right hand side of eq. (8).

In advancing the solution to the next time level, the values of the dependent variables on surfaces with specified flux boundary conditions may be required also. Let $u_s^{n+1/2}$ denote the surface value on a typical element edge IJ on the surface, Fig. 1. Following the approach used previously, $u_s^{n+1/2}$ is assumed constant on edge IJ at time $t_{n+1/2}$, but at time t_n , u , E , F and H vary along the edge. Thus the following approximations are used on an element edge

$$u(x, y, t_{n+1/2}) = u_s^{n+1/2} \quad (9a)$$

$$u(x, y, t_n) = [N(s)]\{u\}^n \quad (9b)$$

$$E(x, y, t_n) = [N(s)]\{E\}^n \quad (9c)$$

$$F(x, y, t_n) = [N(s)]\{F\}^n \quad (9d)$$

$$H(x, y, t_n) = [N(s)]\{H\}^n \quad (9e)$$

where $[N(s)]$ denotes the interpolation functions. Using the method of weighted residuals, the values for $u_s^{n+1/2}$ are derived by integrating along the length L of an element edge. Hence

$$\begin{aligned} L u_s^{n+1/2} &= \int_L [N] ds \{u\}^n - \frac{\Delta t}{2} \int_L \left[\frac{\partial N}{\partial x} \right] ds \{E\}^n \\ &\quad - \frac{\Delta t}{2} \int_L \left[\frac{\partial N}{\partial y} \right] ds \{F\}^n + \frac{\Delta t}{2} \int_L [N] ds \{H\}^n. \end{aligned} \quad (10)$$

Thus, eqs. (8) and (10) can be used to advance explicitly the element and surface values of the dependent variables to $t_{n+1/2}$. Beginning with nodal values of $\{u\}^n$, $\{E\}^n$, $\{F\}^n$ and $\{H\}^n$, eq. (8) is used to compute constant values $u_D^{n+1/2}$ for each element. In a similar way, eq. (10) is used to compute constant surface values $u_s^{n+1/2}$ for element boundary edges that require these values at $t_{n+1/2}$. These values are computed explicitly by looping through all elements and appropriate element edges.

Time Level t_{n+1}

To advance the solution to t_{n+1} , forward and backward truncated Taylor series expansions

at $t^{n+1/2}$ are used to write the approximation

$$u(x, y, t_{n+1}) = u(x, y, t_n) + \Delta t \frac{\partial u}{\partial t}(x, y, t_{n+1/2}). \quad (11)$$

Then, following the approach used previously, eq. (4) is introduced on the right side to yield

$$u(x, y, t_{n+1}) = u(x, y, t_n) - \Delta t \left[\frac{\partial E}{\partial x}(x, y, t_{n+1/2}) + \frac{\partial F}{\partial y}(x, y, t_{n+1/2}) \right] \quad (12)$$

$$- \Delta t H(x, y, t_{n+1/2}).$$

$$+ \Delta t \left[\frac{\partial E}{\partial x}(x, y, t_{n+1/2}) + \frac{\partial F}{\partial y}(x, y, t_{n+1/2}) \right]$$

$$+ \Delta t H(x, y, t_{n+1/2}).$$

The equation for the nodal values of $\{u\}^{n+1}$ can next be derived by the method of weighted residuals using the interpolation functions N_i as weighting functions. These terms containing the derivatives are integrated by parts. The resulting equation contains values of the fluxes E and F evaluated at $t_{n+1/2}$. The fluxes at the mid-step are linearly interpolated from their values at t_n and t_{n+1} . Thus

$$E(x, y, t_{n+1/2}) = (1-\theta) E(x, y, t_n) + \theta E(x, y, t_{n+1}) \quad (13)$$

$$F(x, y, t_{n+1/2}) = (1-\theta) F(x, y, t_n) + \theta F(x, y, t_{n+1})$$

where the interpolation parameter θ varies from zero to one. These operations yield the equations for the nodal values of a single element,

$$[M]\{u\}^{n+1} = [M]\{u\}^n + (1-\theta)\{R_1\}^n + (1-\theta)\{R_2\}^n + \theta\{R_3\}^{n+1} + \theta\{R_4\}^{n+1} + \{R_5\}^{n+1/2} \quad (14)$$

where

$$[M] = \int_A \{N\}\{N\} dA \quad (15a)$$

$$\{R_1\}^n = \Delta t \int_A \left\{ \frac{\partial N}{\partial X} \right\} [N] dA \{E\}^n \quad (15b)$$

$$+ \Delta t \int_A \left\{ \frac{\partial N}{\partial Y} \right\} [N] dA \{F\}^n$$

$$\{R_2\}^n = - \Delta t \int_S \{N\} [N] ds (\lambda \{E\}_S^n) \quad (15c)$$

$$+ m \{F\}_S^n$$

$$\{R_3\}^{n+1} = \Delta t \int_A \left\{ \frac{\partial N}{\partial X} \right\} [N] dA \{E\}^{n+1} \quad (15d)$$

$$+ \Delta t \int_A \left\{ \frac{\partial N}{\partial Y} \right\} [N] dA \{F\}^{n+1}$$

$$\{R_4\}^{n+1} = - \Delta t \int_S \{N\} ds (\lambda \{E\}_S^{n+1}) \quad (15e)$$

$$+ m(F)_S^{n+1}$$

$$\{R_5\}^{n+1/2} = \Delta t \int_A \{N\} dA H^{n+1/2} \quad (15f)$$

In eqs. (15c) and (15e) the coefficients λ and m are the components of a unit vector normal to the boundary, see Fig. 1. Following usual finite element procedures, the element matrices given in eq. (15) are assembled to form system equations.

The matrix $[M]$ defined by eq. (15a) is the element consistent mass matrix. The terms $\{R_i\}$, $i = 1, 2, \dots, 5$, defined by eqs. (15b - 15f) represent "load" vectors. The load vectors $\{R_1\}^n$ and $\{R_2\}^n$ are computed from value known at time step t_n ; the load vector $\{R_5\}^{n+1/2}$ is computed from values computed at time step $t_{n+1/2}$. The load vectors $\{R_3\}^{n+1}$ and $\{R_4\}^{n+1}$ depend on values yet to be determined at t_{n+1} . The consistent mass matrix and the latter two load vectors mean that the algorithm in the general form of eq. (14) with arbitrary θ is an implicit scheme. For the computations presented in this paper, the algorithm was cast into an explicit form by using a lumped mass matrix and selecting $\theta = 0$ to eliminate $\{R_3\}^{n+1}$ and $\{R_4\}^{n+1}$.

The explicit two time-level Taylor-Galerkin algorithm is conditionally stable. Guidelines for determining allowable time steps have been established by studying linear one-dimensional model equations selected to represent the mathematical character of the physical problems. An analysis of the coupled thermo-elasticity problem shows that the partial differential equations are hyperbolic. The stability of the algorithm was studied by considering the linear equation.

$$\frac{\partial u}{\partial t} + a \frac{\partial u}{\partial x} = D \frac{\partial^2 u}{\partial x^2} \quad (16)$$

where a is a propagation speed, and D is a diffusion coefficient. A stability analysis of the algorithm applied to

this equation shows that the time step should satisfy

$$\Delta t < \frac{\Delta x}{1 + 2/\frac{\partial \Delta x}{D}} \quad (17)$$

where Δx is the mesh spacing. An analysis of the quasistatic thermal-structural problem shows that the partial differential equations are parabolic. The stability of the algorithm was studied by considering the linear parabolic equation,

$$\frac{\partial u}{\partial t} = D \frac{\partial^2 u}{\partial x^2} \quad (18)$$

A stability analysis of the algorithm applied to this equation shows that the time step should satisfy

$$\Delta t < \frac{\Delta x^2}{2D} \quad (19)$$

For practical computations, eqs. (17) and (19) have been used as a guide to estimate the time step, but insight into the physical problem and some trial and error have been needed to perform the computations successfully.

Explicit Evaluation of Element Integrals

Element integrals for the Taylor-Galerkin algorithm shown in eqs. 8, 10, and 15 were evaluated in closed form¹ to avoid numerical integrations that are customary for quadrilateral elements. The approach was also used for the closed form evaluation of three dimensional hexahedral element integrals². The CPU time used by the closed form evaluation of the element integrals has been investigated and compared with CPU times required for different orders of Gauss numerical integration for quadrilateral and hexahedral elements. For the quadrilateral elements, the CPU time required to evaluate all element integrals is reduced by a factor of about 50. For hexahedral elements, the time savings are even more significant. Although these time savings are beneficial, the CPU time required for element integral evaluation normally represents less than about 10% of the total CPU time required for the solution.

Vector Programming Strategies

The Taylor-Galerkin algorithm was implemented with vectorization strategies specifically for the Langley VPS 32 (a Cyber 205 with 32 million words of central memory). This computer achieves high computational speed when performing operations on long vectors. Vector lengths of at least 60 are required to justify vectorization efforts with maximum payoff achieved for vector lengths of 1000 or more. The predominant vector lengths in the

vectorization scheme are the number of elements in the finite element model with occasional operations using vector lengths equal to the number of nodes.

The critical vectorization tasks are for operations that are repetitive and performed at every time step. For finite element algorithms, these operations are: (1) assembly of element contributions into the global system of equations, (2) solution of the global system of equations, and (3) application of boundary conditions.

The assembly of element contributions into the global system of equations requires special routines for vectorization. Nodal unknowns are stored in one dimensional arrays from 1 to the number of nodes in the model, and in general, node numbering may be arbitrary throughout the mesh. Assembly of element contributions is performed using the VPS 32 FORTRAN-supplied scatter routine which places an element contribution into the proper location in the system of equations based on the element connectivity. Every element that contains a particular node in its connectivity provides its own contribution to the system equations, therefore, the assembly is an additive operation. "Scattering" alone would merely overwrite a previous element contribution. The special vector routine, then does an "additive scatter."

For an explicit scheme, solutions are obtained directly, so that operation (2) vectorizes naturally. Operation (3), the application of boundary conditions, is an intrinsically scalar operation and difficult to vectorize. However, use of bit vectors to flag boundary nodes and use of VPS 32 FORTRAN supplied routines enables full vectorization of this operation.

A program flow chart for the Taylor-Galerkin algorithm is shown in Fig. 2. Note that the element integrals are computed once and stored for later use in the transient loop. The Lapidus smoothing¹⁻² represents artificial damping used to reduce spurious oscillations. The smoothing is typically used only in the vicinity of discontinuities, e.g. shock fronts, in the solution.

Application

Two applications are presented to validate and illustrate the basic capabilities of the approach. The first application is a one-dimensional, transient, linear thermal-stress problem for which an exact solution is available. The second application is a quasistatic, nonlinear, two-dimensional thermal-stress problem of a cylinder subject to aerodynamic heating.

Thermal Stresses in an Elastic Half-Space

The problem (see Figure 3) consists of an elastic half-space $x>0$ with the plane $x=0$ free of stress, and the medium constrained so that the only displacements occur in the x direction. The plane $x=0$ is suddenly at time equal zero exposed to convective heating through a convection coefficient h . The thermal-mechanical coupling term in eq. (1c) is neglected to facilitate obtaining an exact solution.

The problem was solved using the two-step Taylor-Galerkin algorithm with two meshes (Fig. 3) of quadrilateral elements. Quadrilateral elements are not required since the problem is one-dimensional, but this application served to validate the quadrilateral elements and the vector code used for the second application. The temperature and stress distributions computed for 100 and 500 elements are compared with the exact solution in Figs. 4 and 5, respectively.

The computed temperature coincides with the exact solution for both meshes. The refined mesh was needed to resolve the sharp peak in the propagating stress shown in Fig. 5. The coarse mesh predicts a smooth stress distribution but rounds the sharp peak significantly underestimating the peak values. The refined mesh solution shows that the solution is converging accurately to the exact solution as the mesh is refined.

The problem illustrates the basic capability of the algorithm for accurately solving transient thermal-stress problems with propagating disturbances. Computational times for this relatively small problem are modest compared to CFD problems.

Cylinder Subject to Aerodynamics Heating

The problem (Fig. 6) concerns the thermal-structural response of a stainless steel cylinder subject to highly-localized aerodynamic heating due to supersonic flow. The problem simulates the type of aerodynamic heating that may occur on leading edges of engine structures in hypersonic flight vehicles. The heating is time-dependent and results from the interaction of two shocks in the flow-field. For $0 < t < 1$ s, the cylinder is heated symmetrically by a supersonic flow that causes a symmetric bow shock to form in front of the cylinder leading edge. For $1 < t < 2$ s, an oblique shock is introduced into the flow by rotating the wedge shown in Fig. 6. The wedge-induced shock and the bow shock then intersect forming a localized region of heating at about 10° below the cylinder horizontal centerline. Wind tunnel experiments suggest that the resulting heating can be quite severe. The heating may be represented approximately using the convective coefficients shown in Fig. 7. The heating distribution is modeled using two superimposed cosine distributions. The maximum localized heating for $1 < t < 2$ s is about an order of magnitude greater than the heating for $0 < t < 1$ s.

Over the temperature range that occurs in the cylinder, the thermal and structural properties of the stainless steel cylinder vary significantly. The specific heat, thermal conductivity and coefficient of thermal expansion increase linearly as shown in Fig. 8. In addition, the stress-strain behavior for the material alters significantly with temperature as shown in Fig. 9 where it can be seen that the elastic modulus and yield strength decrease with increasing temperature.

The finite element model of the cylinder with the thermal and structural boundary conditions is shown in Fig. 10. A graded mesh of 1500 elements and 1596 nodes is used to model one-half of the cylinder. The model represents convective heating on the leading edge, and assumes negligible heat loss on the other cylinder surfaces. The cylinder external surfaces are stress-free, but the rigid body motion of the cylinder is prohibited by the three specified zero displacements shown. Since the duration of the heating is much larger than the propagation times for thermal-stress waves, an excellent approximation is to neglect structural inertia effects and perform a quasistatic analysis. Thus eqs. (3a) are solved by the Taylor-Galerkin algorithm. The temperature response is computed in a time-accurate manner, but the corresponding stress problem is solved independently using the fictitious damping constant to march the structural response to a steady-state solution for a temperature distribution computed at a given time.

The thermal-structural response of the cylinder was computed for two cases: (1) constant material properties, and (2) temperature-dependent properties. Comparative temperature distributions for $t=1$ s and $t=2$ s are presented in Figs. 11-12, respectively. The corresponding stress distributions superimposed on greatly exaggerated deformed structures are shown in Figs. 13-14.

The temperatures distribution at $t=1$ s (Fig. 11) is changed only slightly by the temperature-dependent properties, but the temperature distributions at $t=2$ s (Fig. 12) differ considerably. For $1 < t < 2$ s, the high local heating raises the temperatures near the surface significantly. The increasing conductivity and specific heat in the temperature-dependent properties analysis produce smaller gradients and a much lower surface temperature. The stress-distribution and deformations of Figs. 13 and 14 reflect two temperature-dependent property effects. The first effect is due to the differences in the computed temperatures, and the second is due to the difference in the stress-strain behavior of the material. Fig. 14, in particular, shows these effects dramatically. For the constant property case, Fig. 14a shows an excessively large compressive stress (-325 ksi) well above the material's allowable stress. Fig. 14b, shows more realistic behavior with smaller deformations and stress levels (-150 ksi) still high but at acceptable levels. These lower levels reflect the reduced temperatures and the

inelastic deformations permitted by the nonlinear stress-strain curves (Fig. 9).

This problem reflects some of the computational advantages of the explicit Taylor-Galerkin algorithm for realistic thermal-structural problems. The algorithm is highly vectorizable and very large problems can be solved on a supercomputer because global stiffness matrices are not formed. Non-linear property behavior is included conveniently through the vectors {E} and {F} independent of element stiffness matrices. Element matrices are computed from closed-form equations and can be computed outside of the transient loop and stored for later use. Principal disadvantages of the algorithm include its conditional stability and tendency to produce oscillatory solutions in the presence of sharp solution discontinuities. These disadvantages have been encountered in inviscid flow computations¹⁻² and nonlinear thermal-structural applications with propagating shock waves may show similar results. Further computations are needed to investigate these possibilities. Another area worthy of further study is methods for accelerating the convergence of the time-marching solution to the steady-state structural equilibrium problem associated with quasistatic thermal-structural analysis.

Concluding Remarks

A Taylor-Galerkin finite element solution algorithm for transient nonlinear thermal-structural analysis of large, complex structural problems is described. The two-step Taylor-Galerkin algorithm is an application of an algorithm recently developed for problems in compressible fluid dynamics. Two thermal-structural formulations are described. The first formulation is for thermal-structural problems where a mechanical coupling term is present in the heat transfer energy equation and the inertial terms are retained in the structural equations of motion. The second formulation is for a quasistatic problem where thermal-mechanical coupling and structural inertia terms are neglected. Solutions to transient and equilibrium problems are obtained by time-marching. For a lumped mass approach, the algorithm is conditionally stable. The algorithm has been implemented on the VPS-32 vector computer with special programming strategies to yield very high computational speeds.

Two applications of the algorithm to thermal-structural problems are presented. The first application is a one-dimensional, transient linear thermal-stress problem for an elastic half-space. Comparisons of finite element predictions with an exact solution validate the approach and illustrate the capability to capture propagating stress waves accurately. The second application is a quasistatic, nonlinear two-dimensional thermal-stress problem of a cylinder subject to high localized aerodynamic heating. Comparisons of constant material property and variable property

solutions illustrated the importance of nonlinear effects in realistic problems and the capability of the algorithm to incorporate the nonlinearities effectively.

The applications have validated the fundamental capabilities of the algorithm for two basic thermal-structural formulations. Additional study is needed for more demanding transient, nonlinear thermal-stress problems. Further experience is needed also for quasistatic problems particularly with methods to accelerate the convergence of the steady-state structural problem. Since the algorithm can be applied to fluid, thermal and structural problems there is potential for developing, with one methodology, the capability for integrating these analyses into a single program. Such an integrated methodology will permit the first computational solution to problems with strong fluid-thermal-structural interactions. The development of an integrated fluid-thermal-structural analysis capability is a current research goal.

Acknowledgement

We are pleased to acknowledge the support of the NASA Langley Aerothermal Loads Branch and the advice and encouragement of Allan R. Wieting our technical monitor. We are also pleased to acknowledge the support of the Air Force Wright Aeronautical Laboratories and the guidance of Donald B. Paul our technical monitor at Wright-Patterson.

References

1. Bey, Kim S., Thornton, Earl A., Dechaumphai, Pramote, and Ramakrishnan, Ramki: "A new Finite Element Approach for Prediction of Aerothermal Loads-Progress in Inviscid Flow Computations," Proceedings of the 7th AIAA Computational Fluid Dynamics Conference, Cincinnati, OH, July 15-17, 1985.
2. Thornton, Earl A., Ramakrishnan, Ramki and Dechaumphai, Pramote: "A Finite Element Approach for Solution of the 3D Euler Equations", AIAA 24th Aerospace Science Meeting, Reno, Nevada, January 6-9, 1986, AIAA-86-0106.
3. Nowinski, J. L.: Theory of Thermoelasticity with Applications, Sijthoff and Noordhoff International Publishers, 1978.
4. Huebner, K. H. and Thornton, E. A.: The Finite Element Method for Engineers, Second Edition, John Wiley, New York, 1982.

ORIGINAL PAGE IS OF POOR QUALITY

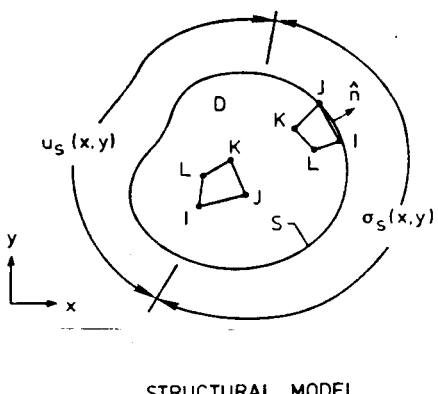
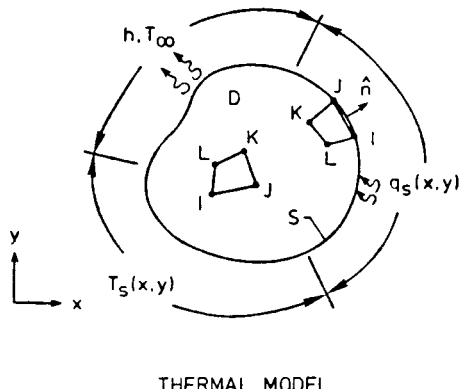


Fig. 1 Two dimensional finite element thermal-structural model.

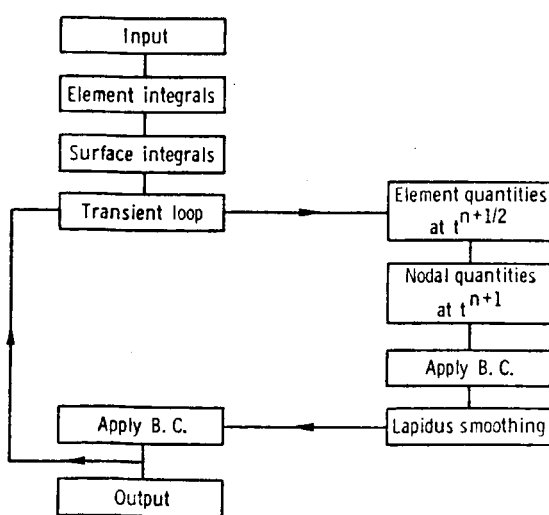
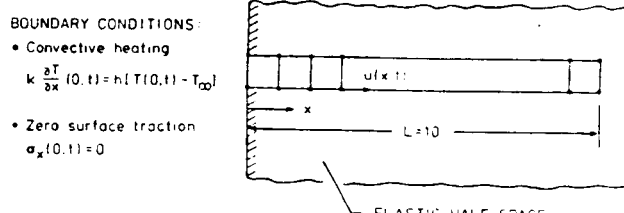


Fig. 2 Program flowchart for Taylor-Galerkin algorithm.



INITIAL CONDITIONS:

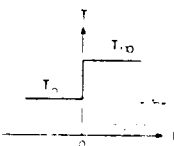
 $T(x,0) = T_0$
 $u(x,0) = 0$
 $\dot{S}(x,0) = 0$


Fig. 3 Transient thermal stress in an elastic half space.

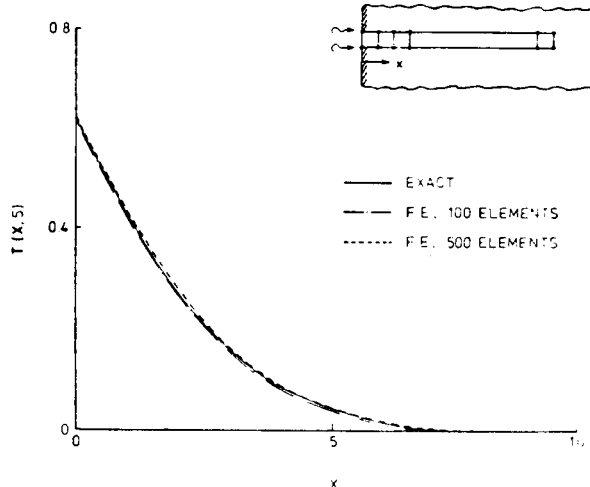


Fig. 4 Comparative temperature distribution at time $t = 5$.

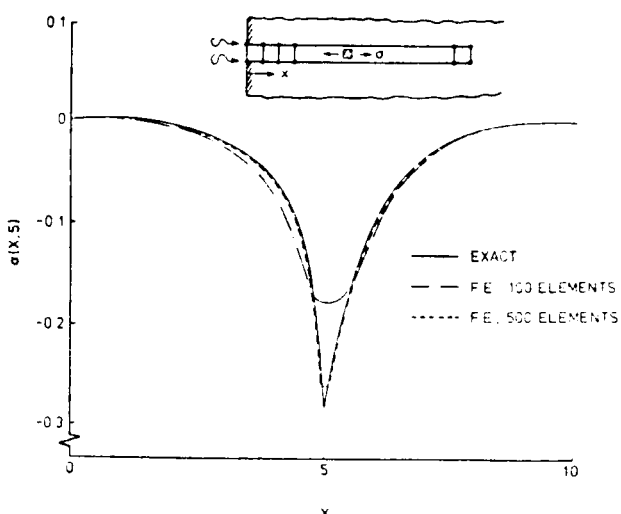


Fig. 5 Comparative thermal stress distributions at time $t = 5$.

ORIGINAL PAGE IS
OF POOR QUALITY

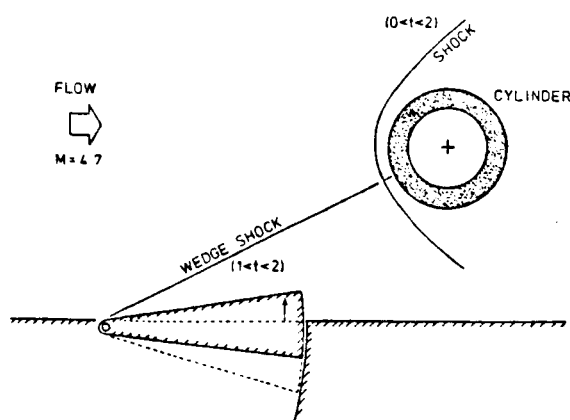


Fig. 6 Thermal-structural analysis of a cylinder under shock wave heating.

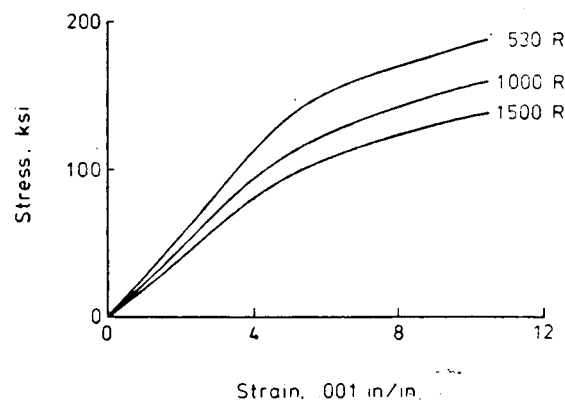


Fig. 9 Temperature dependent stress-strain curves of cylinder.

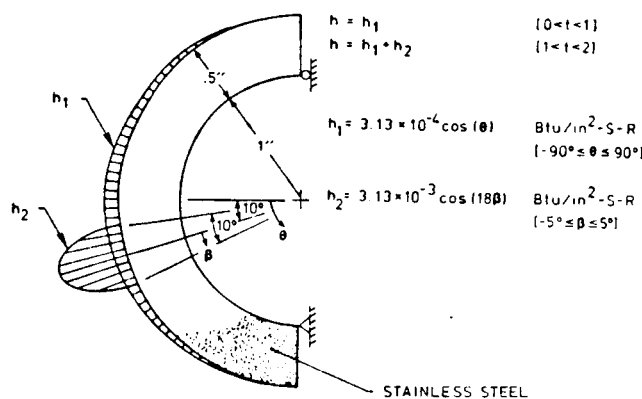


Fig. 7 Convective coefficient distributions on cylindrical surface.

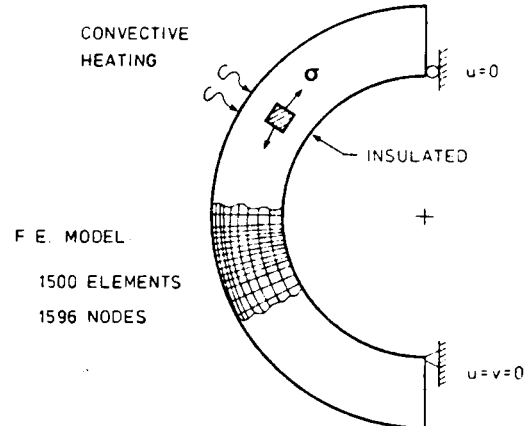


Fig. 10 Finite element thermal-structural model for cylinder.

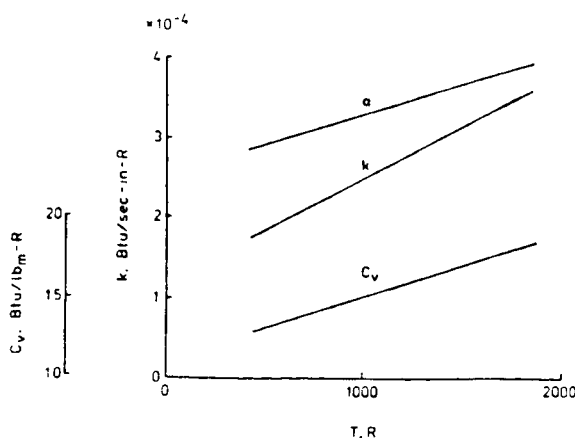


Fig. 8 Temperature dependent material properties of cylinder.

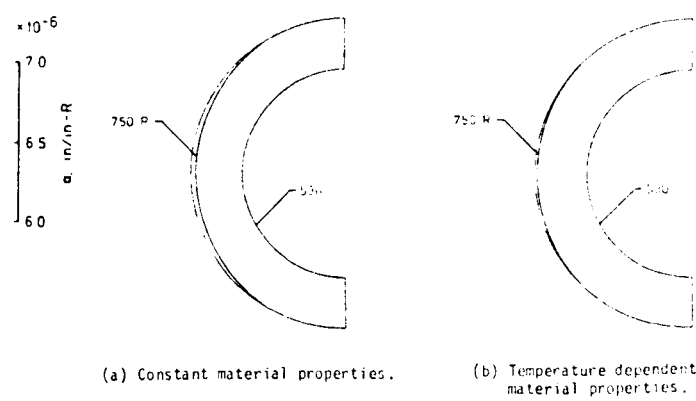
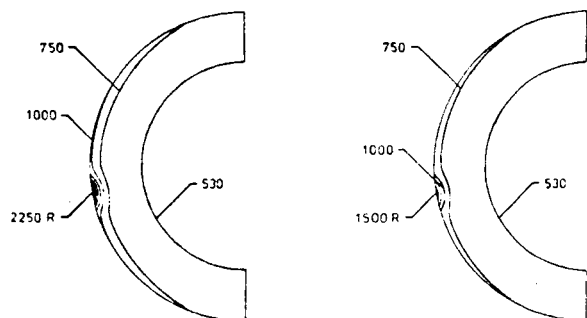


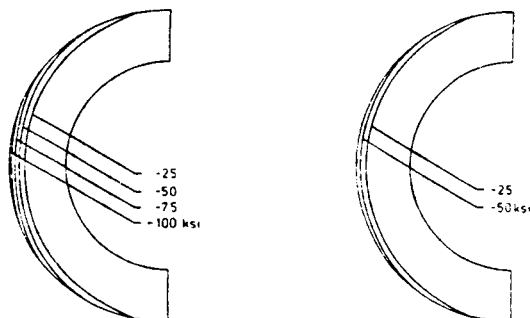
Fig. 11 Comparative temperature distributions (in R) at 1 second.

ORIGINAL PAGE IS
OF POOR QUALITY



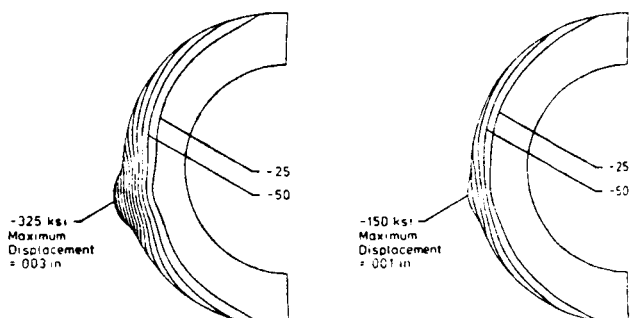
(a) Constant material properties. (b) Temperature dependent material properties.

Fig. 12 Comparative temperature distributions (in R) at 2 seconds.



(a) Constant material properties, (b) Temperature dependent material properties, Elastic analysis.

Fig. 13 Comparative circumferential stress distributions (in ksi) at 1 second.



(a) Constant material properties, (b) Temperature dependent material properties, Elastic analysis.

Fig. 14 Comparative circumferential stress distributions (in ksi) at 2 seconds.